Vaccine monitoring shows that focused immunization with SARS-CoV-2 receptor-binding domain provides a better neutralizing antibody response than full-length spike protein

Rafael Bayarri-Olmos (✉ rafael.bayarri.olmos@regionh.dk)
Rigshospitalet, Faculty of Health and Medical Sciences, University of Copenhagen
https://orcid.org/0000-0003-3202-9679

Manja Idorn
Department of Biomedicine, Aarhus Research Center for Innate Immunology, Aarhus University

Anne Rosbjerg
Rigshospitalet, Faculty of Health and Medical Sciences, University of Copenhagen

Laura Pérez-Alós
Rigshospitalet, Faculty of Health and Medical Sciences, University of Copenhagen
https://orcid.org/0000-0002-0368-4976

Cecilie Hansen
Rigshospitalet, Faculty of Health and Medical Sciences, University of Copenhagen

Laust Johsen
Novo Nordisk A/S

Charlotte Helgstrand
Novo Nordisk A/S

Fredrik Kryh Öberg
Novo Nordisk A/S https://orcid.org/0000-0002-7089-2118

Max Søgaard
4ExpreS2ion Biotechnologies

Søren Paludan
Aarhus University https://orcid.org/0000-0001-9180-4060

Theresa Bak-Thomsen
Novo Nordisk A/S

Joseph Jardine
IAVI Neutralizing Antibody Center, Scripps Research

Mikkel-Ole Skjoedt
Institute of Immunology and Microbiology, University of Copenhagen

Peter Garred
University of Copenhagen, Copenhagen https://orcid.org/0000-0002-2876-8586

Article

Keywords: SARS-CoV-2, RBD, spike, neutralizing antibodies, vaccine, monoclonal antibodies

Posted Date: January 4th, 2021

DOI: https://doi.org/10.21203/rs.3.rs-134388/v1

Vaccine monitoring shows that focused immunization with SARS-CoV-2 receptor-binding domain provides a better neutralizing antibody response than full-length spike protein

Author list: Rafael Bayarri-Olmos[1#], Manja Idorn[2], Anne Rosbjerg[1], Laura Pérez-Alós[1], Cecilie Bo Hansen[1], Laust Bruun Johnsen[3], Charlotte Helgstrand[3], Fredrik Kryh Öberg[3], Max Søgaard [4], Søren R. Paludan[2], Theresa Bak-Thomsen[3], Joseph G. Jardine[5], Mikkel-Ole Skjoedt[1*], and Peter Garred[1*]

Affiliations: [1]Rigshospitalet, Faculty of Health and Medical Sciences, University of Copenhagen, Copenhagen, Denmark; [2]Department of Biomedicine, Aarhus Research Center for Innate Immunology, Aarhus University, Aarhus, Denmark; [3]Novo Nordisk A/S, Måløv, Denmark; [4]ExpreS2ion Biotechnologies, Horsholm, Denmark; [5]IAVI Neutralizing Antibody Center, Scripps Research, La Jolla, California, USA.

*These authors contributed equally.

Running title: Antibody neutralization assay and SARS-CoV-2 vaccine responses

Keywords: SARS-CoV-2, RBD, spike, neutralizing antibodies, vaccine, monoclonal antibodies.

#Corresponding author: Dr. Rafael Bayarri-Olmos, rafael.bayarri.olmos@regionh.dk

Abstract

Effective tools to monitor SARS-CoV-2 transmission and humoral immune responses are highly needed. Protective humoral immunity involves neutralizing antibodies and will be a hallmark for the evaluation of a vaccine response efficacy. Here we present a sensitive, fast and simple neutralization ELISA method to determine the levels of antibody-mediated virus neutralization. We can show that it is strongly correlated with the more elaborate plaque reduction neutralization test (PRNT) ($\rho = 0.9231$, $p < 0.0001$). Furthermore, we present pre-clinical vaccine models using recombinant receptor binding domain (RBD) and full-length spike antigen as immunogens showing a profound antibody neutralization capacity that exceeds the highest neutralization titers from convalescent individuals. Using a panel of novel high-affinity murine monoclonal antibodies (mAbs) we also show that majority of the RBD-raised mAbs have inhibitory properties while only a few of the spike-raised mAbs do. In conclusion, the ELISA-based viral neutralization test offers a time- and cost-effective alternative to the PRNT. The immunization results indicate that vaccine strategies focused only on the RBD region may have major advantages over those based on the full spike sequence.

Introduction

COVID-19 has within a short time become a worldwide health crisis and the scientific community has stepped up in earnest to this unprecedented challenge to develop diagnostic and therapeutic tools to contain and treat the pandemic. As of September 2020, there were 231 vaccine candidates in the pipeline and more than 30 in clinical trials[1]. Apart from vaccines to prevent SARS-CoV-2 infection, passive anti-SARS-CoV-2 antibody therapy to treat COVID-19 patients has emerged as a treatment possibility[2]. Studies have reported that the majority of COVID-19 patients develop neutralizing antibodies targeting the spike glycoprotein within the first two weeks after symptom onset[3–7], and that SARS-CoV-2-derived antibodies have a protective effect in COVID-19 animal models such as rhesus macaques[8] and rodents[9–12]. Overall, current reports support the idea that antibody-based immunotherapy in the form of monoclonal antibodies (mAbs) is beneficial in the treatment of COVID-19 patients. At the same time, the use of convalescent plasma therapy has become debated[13,14]. Nevertheless, protective humoral immunity involves neutralizing antibodies and will be a hallmark for the evaluation of a vaccine response efficacy.

The current standard method to evaluate the presence of neutralizing antibodies in the blood is the plaque reduction neutralization test (PRNT). While it remains the gold standard due to its specificity and sensitivity[15–18], the PRNT is labour- and time-intensive, difficult to standardize, and requires highly specialized personnel in high biosafety levels laboratories. Thus, it is of critical importance to develop reliable and convenient methods to assess the virus-neutralizing capacity of patient- or animal-derived antibodies to select convalescent plasma donors, develop mAbs-based therapeutics, and evaluate the efficacy of vaccination strategies.

Here we describe the development of a quick, sensitive, and easy-to-operate neutralization ELISA-based test for the determination of neutralizing antibodies based on the interaction between recombinant human ACE-2 ectodomain and the SARS-CoV-2 RBD. We benchmarked our assay with the PRNT and two commercially available tests. Using a previously described cohort of PCR-confirmed COVID-19 convalescent patients[19], we measured the neutralization potency and the relative titers of IgG, IgM, and IgA against the RBD, spike, and protein N. Furthermore, we evaluated the vaccine responses in pre-clinical vaccine animal models using our antibody neutralization ELISA and generated high-affinity monoclonal antibodies against the RBD and full-length spike protein. Finally, we performed binding kinetic characterization, epitope binning, and determined their neutralization potency in our antibody neutralization ELISA and the PRNT.

Materials and methods

Buffers

The following buffers were used: PBS (10.1 mM disodium phosphate, 1.5 mM monopotassium phosphate, 2.7 mM potassium chloride, 137 mM sodium chloride), PBS-T (PBS + 0.05 % Tween-20), PBS-T-EDTA (PBS-T + 5 mM EDTA), sample buffer (PBS-T-EDTA + 5% skim milk [70166 Merck, New Jersey, USA]).

Production and purification of recombinant ACE-2 ectodomain and SARS-CoV-2 viral proteins

The nucleotide sequence corresponding to the human ACE-2 receptor (aa. 17–740) with an N-terminal CD33 signal peptide and a dual C-terminal 10xHis-AviTag (HHHHHHHHHH-GLNDIFEAQKIEWHE) was ordered from Twist Biosciences and subcloned into a pTT5 expression vector. Recombinant ACE-2 protein was produced by transient transfection using the Expi293™ Expression System Kit (Gibco, Thermo Fisher Scientific, Massachusetts, USA) according to the manufacturer's recommendations and grown shaking in suspension in a humidified incubator at 37 °C and 8% CO_2. On day five after transfection, AmMag™ Ni Magnetic Beads (GenScript, New Jersey, USA) were added to the cell culture, followed by 2 h of additional incubation. The magnetic beads were subsequently removed from the cell culture, washed, and eluted according to the manufacturer's instructions. The purified protein was buffer exchanged into 50 mM Hepes, pH 7.4, 150 mM NaCl. The nucleotide sequence for the trimeric prefusion-stabilized spike protein ectodomain (QIC53204, aa. 1–1208) was optimized in terms of the codon adaptation index, high 5' mRNA folding energy, and repeated adjacent codons. The coding sequence was modified by including two stabilizing proline substitutions in positions 986–987, a GSAS substitution at the furin cleavage site (aa. 682–685), and a C-terminal trimerization domain-8xHis (YIPEAPRDGQAYVRKDGEWVLLSTFL-HHHHHHHH)[20]. All DNA manipulations were done in Visual Gene developer 1.9[21]. The nucleotide sequence was synthesized by GeneArt (Thermo Fisher Scientific) and subcloned into a pcDNA3.4 expression vector. The production and purification of SARS-CoV-2 protein N, RBD, and trimeric prefusion-stabilized spike protein ectodomain used for immunization[19]. Purified RBD was biotinylated with a biotin ligase kit (Avidity, Colorado, USA) according to the manufacturer's instructions. The plasmid used for synthesizing the SARS-CoV-2 RBD polypeptide was made and kindly contributed by the International AIDS Vaccine Initiative ("IAVI") and provided by the responsible IAVI employee, Joseph Jardine (Scripps Institute, La Jolla, California, USA). The nucleotide sequence for the monomeric prefusion-stabilized spike protein ectodomain (aa. 16–1208), modified with an N-terminal BiP signal peptide, two proline substitutions (aa. 967, 987) an AARA substitution at the furin cleavage site, and a C-terminal Capture select C tag (Thermo Fisher Scientific), was synthesized and subcloned into a pExpreS2-1 (ExpreS^{2}ion Biotechnologies) vector by GeneArt. Transiently transfected Drosophila melanogaster S2 cells (ExpreS^2 Cells, ExpreS^{2}ion Biotechnologies) were grown shaking in suspension at 25 °C for three days after which the supernatant was harvested by centrifugation, concentrated and buffer exchanged approximately 10-fold. The protein was purified on a Capture Select C-tag XL column (Thermo Fisher

Scientific) eluted using $MgCl_2$ (0.5–1 M), followed by size exclusion chromatography using a Superdex200 column (Cytiva, Massachusetts, USA) equilibrated in PBS.
Protein purity was confirmed by SDS gel electrophoresis and Instant Blue total protein stain (Abcam, Cambridge, UK), while the identity of the purified proteins was confirmed by blotting unto Invitrolon PVDF membranes (Invitrogen, Thermo Fisher Scientific) and detecting either with anti-hACE-2 goat IgG (AF933 R&D systems, Minnesota, USA) followed by anti-sheep-HRP conjugate polyclonal rabbit 1.3 g/L (P0163 Dako, Agilent, California, USA) or with streptavidin-HRP conjugate (RPN131V Amersham, Sigma-Aldrich, Missouri, USA).

Serum and plasma samples

A total of 310 serum and plasma samples from recovered individuals with a previous SARS-CoV-2 infection confirmed by qPCR were included in the study. The participants have been described elsewhere[19]. Serum and plasma samples from healthy blood donors collected before December 2019 were used as negative control.

Development of an ELISA-based SARS-CoV-2 neutralization assay

The assay was optimized by sequentially assessing the effect of detection reagents, i.e. high sensitivity streptavidin-HRP (HS-strep-HRP, 21130 Pierce, Wisconsin, USA) or streptavidin-HRP conjugate (RPN131V Amersham); convalescent serum pre-incubation times (0–60 min); ACE-2 coat concentration (0.5–8 µg/ml); RBD:ACE-2 binding times (15–90 min); and sample choice (serum, heat-inactivated serum, plasma). In the final setup, ACE-2 (1 µg/ml) was coated in MaxiSorp microtiter plates (Thermo Fisher Scientific) overnight in PBS at 4 °C. The day after, biotinylated RBD (4 ng/ml) was incubated with HS-strep-HRP (1:16,000 dilution) and convalescent serum dilutions (6-point 4-fold dilution starting at 20%) for 60 min in low-binding polypropylene round-bottom plates (Thermo Fisher Scientific). Next, the serum:RBD mix was transferred to ACE-2 coated plates and allowed to bind for 15 min, before detection with TMB One (KemEnTec Diagnostics, Taastrup, Denmark). The reaction was stopped with 0.3 M H_2SO_4 and the optical density (OD) measured at 450 nm. Microtiter plates were washed thrice with PBS-T between steps and all incubations took place at room temperature (RT) in an orbital shaker unless otherwise stated. The neutralization index was calculated as: $Neutralization\ (\%) = \left(1 - \frac{sample\ OD}{control\ OD}\right) * 100$. Negative neutralization indexes were normalized to 0. A serum pool (n = 3) collected before the emergence of SARS-CoV-2 was used as control. The matrix effects are represented as the ratio between each dilution of serum/plasma/non-specific mAbs and the blank (RBD:HS-strep-HRP in PBS-T) $* 100$. The intra-assay coefficient of variation was calculated on the estimated IC_{50} values of a serum pool from six convalescent patients with high anti-RBD IgG titers measured 8 times in a single plate. The inter-assay coefficient of variation (CV) was calculated on the average IC_{50} of a serum sample with high anti-RBD IgG titers from at least three independent plates run in three different days (n = 12–15).

Plaque reduction neutralization test (PRNT)

SARS-CoV-2, Freiburg isolate, FR-4286 (kindly provided by Professor Georg Kochs, University of Freiburg) was propagated in VeroE6 cells expressing human TMPRSS2 (VeroE6-hTMPRSS2) (kindly provided by Professor Stefan Pöhlmann, University of Göttingen[22]) with a multiplicity of infection (MOI) of 0.05 in DMEM (Gibco, Thermo Fisher Scientific) + 2% FCS (Sigma-Aldrich) + 1% Pen/Strep (Gibco) + L-Glutamine (Sigma-Aldrich) (from here, complete medium). Supernatant from 72 h post-infection containing new virus progeny was harvested and concentrated on 100 kDa Amicon ultrafiltration columns (Merck) by centrifugation at 4,000 x g for 30 min. Virus titer was determined by $TCID_{50\%}$ assay and calculated by Reed-Muench method[23]. Sera from convalescent COVID-19 patients (15 representative samples with low, intermediate, and high RBD-specific IgG titers) was heat-inactivated (30 min, 56 °C), and prepared in 2-fold serial dilutions in complete medium. MAbs raised against SARS-CoV-2 RBD, or prefusion-stabilized spike protein were prepared in complete medium at 100 µg/ml and subsequent 3-fold serial dilution. Serum or antibody dilutions were mixed with SARS-CoV-2 at a final titer of 100 $TCID_{50}$/well and incubated at 4 °C overnight. "No serum" and "no virus" (uninfected) samples were included as controls. The following day virus:serum or virus:antibody mixtures were added to 2 x 10^4 Vero E6-hTMPRSS2 cells seeded in flat-bottom 96-well plates, and incubated for 72 h in a humidified CO_2 incubator at 37 °C, 5% CO_2. The neutralization assay was stopped by fixing with 5% Formalin (Sigma-Aldrich) and staining with crystal violet solution (Sigma-Aldrich). The plates were read using a light microscope (Leica DMi1, Leica, Wetzlar, Germany) with a camera (Leica MC170 HD) at 10x magnification, and the cytopathic effect scored.

Determination of IgG, IgM, and IgA titers against RBD, spike, and protein N

Microtiter 384-well plates were coated with 1 µg/ml of RBD, monomeric full-length spike, or protein N in PBS overnight at 4 °C. Serum samples from COVID-19 convalescent patients were applied in a 3-point 3-fold serial dilution starting at 1:400 in sample buffer. A serum sample from a COVID-19 patient with high IgG, IgM, and IgA titers against RBD was used as a calibrator. HRP-conjugated polyclonal rabbit antibodies against human IgG (P0214), IgM (P0215), and IgA (P0216) (0.5 µg/ml, all from Agilent Technologies, Santa Clara, CA) were used as detection antibodies. Unless otherwise stated, all incubation steps were performed for 1 h at RT in a shaking platform, and the plates were washed between steps with PBS-T. Plates were developed with TMB One for 7 min for IgG, and 10 min for IgM and IgA, and the reaction was stopped with 0.3 M H_2SO_4, and the OD measured as described previously. Antibody titers against RBD have previously been reported by our group[19].

Mice immunization and generation of mAbs against SARS-CoV-2 RBD and spike protein

Four groups (n = 4 per group) of outbred NMRI mice were immunized against SARS-CoV-2 RBD or trimeric prefusion-stabilized spike protein ectodomain. The mice used for mAb generation received three subcutaneous injections with 20 µg of either recombinant RBD or trimeric prefusion-stabilized spike protein ectodomain adsorbed to GERBU P adjuvant (Gerbu, Heilderberg, Germany) as recommended by the manufacturer. Four days before the fusions, the mice received an intravenous boost of 15 µg antigen without adjuvant. Spleenocytes were collected and the fusion was done essentially as described previously[24]. Hybridomas were screened by direct ELISA using MaxiSorp microtiter plates (Thermo Fisher Scientific) coated with 0.5 µg/ml of recombinant monomeric full-length spike protein or RBD and cloned by limiting dilution. Positive clones were purified with HiTrap Protein G columns connected to an Äkta Pure system (both from Cytiva).

For the pre-clinical vaccine strategy, the two other groups (n = 4) of mice received in total four doses of 20 µg recombinant RBD or trimeric full-length spike protein ectodomain as above, and polyclonal antisera were collected seven days after each immunization.

Determination of antibody titers in immunized mice and COVID-19 convalescent patients

Mice sera were applied to microtiter plates coated with RBD or monomeric full-length spike protein (both 1 µg/ml) in a 9-point 4-fold serial dilution starting at 1:100. Human convalescent sera were applied in an 8-point 4-fold serial dilution starting at 1:25. The samples were incubated for 80 min, followed by a 45 min incubation with rabbit anti-mouse-HRP conjugate (1:2000 dilution, P0260) or polyclonal rabbit antibodies against human IgG (0.5 µg/ml, P0214) (both from Agilent Technologies). Development was performed as described previously.

Evaluation of the neutralization potency of mouse serum and mouse-derived mAbs

The neutralization potency was calculated on a 9-point 4-fold serial dilution of serum (starting at a 1:40 dilution) or a 6-point 4-fold dilution of purified mAbs (starting at 24 µg/ml), but otherwise, as described before. Plates were washed between steps with PBS-T and all incubations took place at RT.

Epitope binning and affinity determination of RBD and spike mAbs by Bio-Layer Interferometry (BLI)

Binning experiments were performed using an Octet system (HTX, Red384) (ForteBio, California, USA), based on the principle of BLI, equipped with anti-mouse IgG Fc capture (AMC) sensors (Pall Life Sciences, California, USA), and using the 8-channel mode. The binning

assays were performed using a sandwich setup, and tips were regenerated between each cycle. Antibodies were captured directly from supernatants. Briefly, (1) antibodies were loaded on AMC tips (150 s); (2) AMC tips were blocked with 2 µM of a mix of mouse IgG2a, IgG2b and IgG1 (300s); (3) association with 100 nM spike protein (150s); and (4) competition with second antibodies (150s). Unspecific binding was evaluated by including mouse IgG1 antibody as a first and second antibody control. Response values from the second antibodies from step (4) were used as basis for the binning data, in addition to visual inspection of individual binding curves for all antibody competitions. Running/neutralization buffer was composed of 20 mM Hepes, 150 mM NaCl, 5 mM CaCl2, 0.1% BSA (IgG free), 0.03% Tween-20, pH 7.4. Regeneration buffer was 10 mM glycine-HCl, pH 1.5.

Affinity determination experiments were performed on the same Octet fortebio system instrument as used for the binning experiment. Briefly, (1) antibodies were captured directly from supernatant on AMC sensors (150s), (2) association to serial dilutions of RBD (10-point 2-fold dilution starting at 200 nM) (300s), and (3) a dissociation phase (300s). Reference AMC sensors, loaded with the same specific antibodies as subjected to the RBD concentrations series, were subtracted for each specific antibody before data analysis. Global analysis of association and dissociation phases fitted to a 1:1 binding model were employed.

Ethics

The use of convalescent donor blood sample in this study have been approved by the Regional Ethical Committee of the Capital Region of Denmark with the approval ID: H-20028627.

The animal experimental procedures described in this study have been approved by the Danish Animal Experiments Inspectorate with the approval ID: 2019-15-0201-00090.

Statistics

All analyses were performed with GraphPad Prism 8 (GraphPad Software, California, USA). IC_{50} values were calculated using the equation [inhibitor] vs normalized response with variable slope. IC_{50} values from non-neutralizing serum samples were normalized to 1, and mAbs to 100. The relationship between serum and plasma neutralization index, PRNT vs antibody neutralization ELISA log(IC_{50}), neutralization vs IgG/M/A titers, and neutralization vs RBD affinity was estimated linear regression analyses (goodness of fit reported as R^2) and two-tailed Spearman rank correlation tests. IgG, IgM, and IgA titers were interpolated from a calibrator curve using a four-parameter non-linear curve fitting and reported as AU/ml as described elsewhere[19]. P values < 0.05 were considered statistically significant.

Results

Development of an ELISA-based surrogate virus neutralization test

We synthesized recombinant human ACE-2 ectodomain (aa 17–740) and SARS-CoV-2 RBD (aa 319–591) and purified them by immobilized metal ion chromatography via their C-terminal 10xHis followed by size exclusion chromatography (Figure 1). To avoid steric hindrance between RBD-bound, non-neutralizing antibodies in the analyte and detection antibodies when determining the interaction between ACE-2 and RBD, we biotinylated the latter via a C-terminal AviTag.

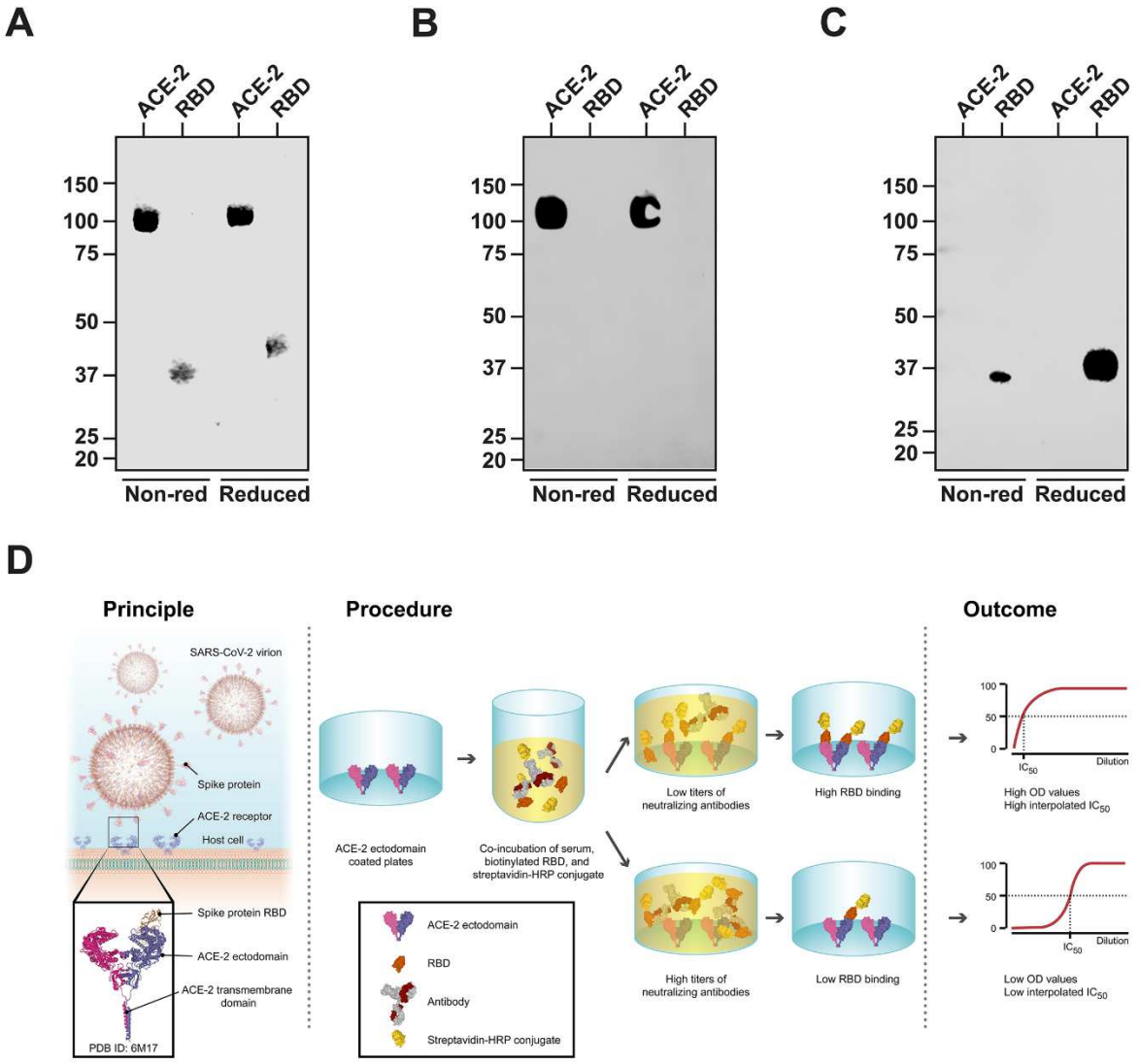

Figure 1. Production of recombinant human ACE-2 and SARS-CoV-2 RBD. Purified ACE-2 and biotinylated RBD are shown by SDS-PAGE total protein stain (A) and western immunoblotting using an anti-ACE-2 antibody (B), or streptavidin-HRP conjugate (C). Schematic representation of the assay setup (D). Virion and protein models were generated with PDBe Molstar from a coarse grain model of the virion[25], the crystal structures of the RBD/ACE-2/B0AT1 complex (PDB ID: 6M17)[26], and a human IgG1 (PDB ID: 1HZH)[27].

Using the recombinant ACE-2 ectodomain and biotinylated SARS-CoV-2 RBD, we developed an ELISA-based neutralization assay defining the reduction of the binding of RBD to coated ACE-2 as a measure for the neutralization potency of sera from convalescent patients or vaccinated mice. Aiming at making this assay as flexible and applicable by other laboratories and testing platforms, we screened the effects of the detection reagents, coat density, assay time, sample matrix, and sample type (Figure 2). Briefly, the ACE-2 coat was titrated and evaluated in terms of the signal-to-noise ratio and total intensity, and a low-density coat of 1 µg/ml was used for further assay development (Figure 2A). Shortening the RBD:ACE-2 incubation time to 15 minutes resulted in the best signal-to-noise ratio, mostly due to a reduction in the background (Figure 2B). Matrix effects were evaluated on serial dilutions of serum, plasma, and non-specific mAb dilutions with acceptable variation (< 20%) over a broad range of concentrations (below 40% serum/plasma and 100 µg/ml mAbs) (Figure 2C). The neutralization potency of matched serum and plasma samples correlated highly ($\rho = 0.9641$, $p < 0.0001$, $n = 108$) (Figure 2D). Heat inactivation of serum and addition of EDTA had no significant effect (Supplementary Figure 1). The intra- and inter-assay CV were found to be satisfactory (4.21% and 12.95%, respectively). Altogether, these results demonstrate that the ELISA-based neutralization test is robust, time-effective, and suitable for the assessment of the neutralization potency in clinical samples.

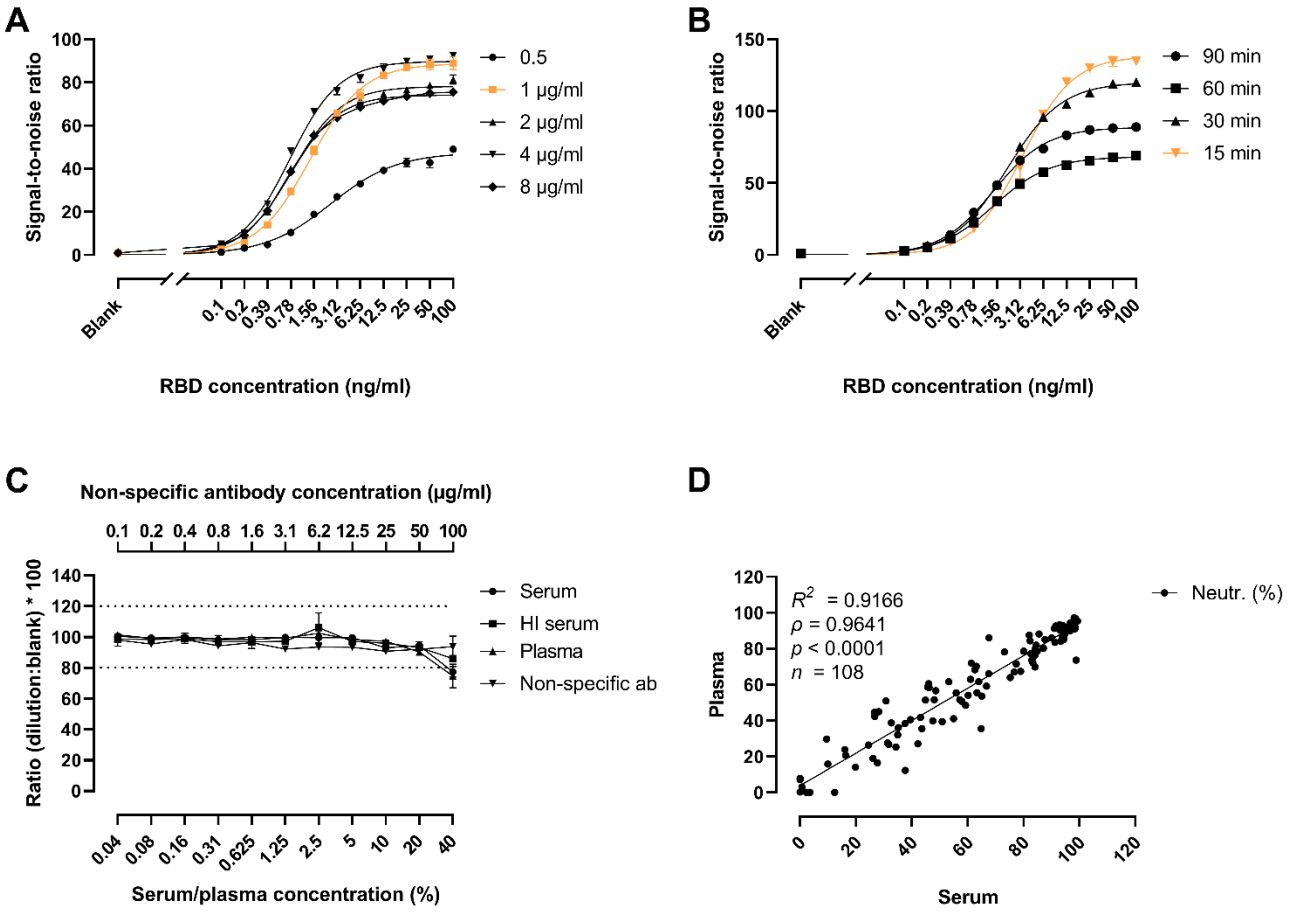

Figure 2. Assay development. Signal-to-noise ratio, calculated as the ratio between a given dilution and the blank, of the binding of serial dilutions of RBD on a 2-fold titration of coated ACE-2 (0.5–8 µg/ml) **(A)**. Signal-to-noise ratio of the binding of serial dilutions of RBD incubated for 15 to 90 min on plates coated with 1 µg/ml of ACE-2 **(B)**. Yellow lines highlight the parameters selected for the final assay setup. The matrix effects were analyzed by co-incubating RBD:HS-strep-HRP in increasing concentrations of a control serum, plasma, or non-specific antibody pools **(C)**. Horizontal dashed lines delimit the 100 ± 20% acceptable recovery range. Spearman rank correlation coefficient between the neutralization (Neutr.) (%) in 20% serum and plasma **(D)**. Trend line represents the linear regression (R^2 = 0.9166).

Assay validation

We compared the performance of the developed antibody neutralization ELISA to an authentic SARS-CoV-2 viral neutralization assay, the PRNT. When categorizing the samples on low, medium, high, and very high neutralization potencies, as calculated by the PRNT, we observed

that the antibody neutralization ELISA results match those obtained by the PRNT (n = 15), with estimated IC_{50} values showing a strong correlation with the PRNT (ρ = 0.9231, n = 12) (Figure 3). Additionally, we benchmarked our antibody neutralization ELISA with two commercially available ELISA-based kits (n = 52). A similarly satisfactory association was observed with two-commercially available neutralization tests (ρ =0.9263–0.9562, R^2 = 0.8445–0.9232, n = 52) (Supplementary Figure 2).

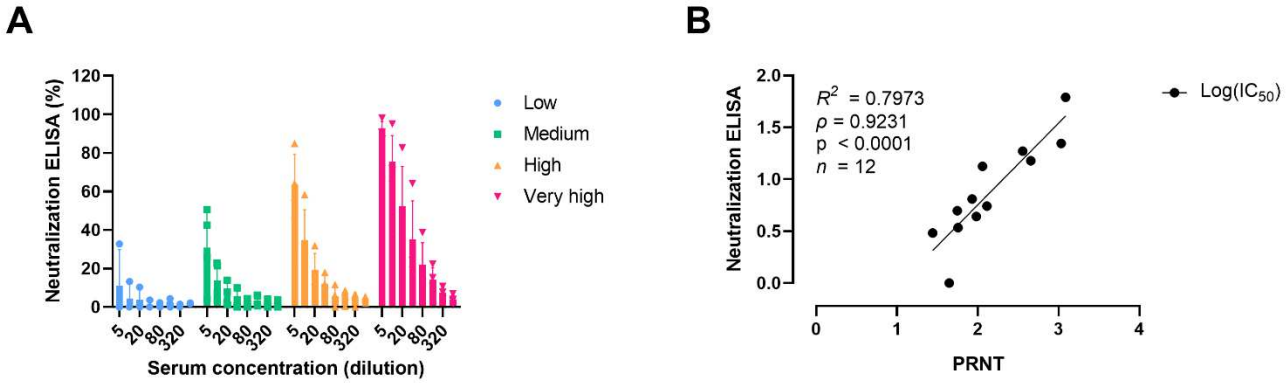

Figure 3. Assay validation. The neutralization potency of COVID-19 convalescent patient sera (n = 15) was determined using the PRNT, classified by low, medium, high, and very high neutralization potency, and analyzed using the developed antibody neutralization ELISA **(A)**. IC_{50} values were calculated from the neutralization indexes obtained from both tests using the equation [inhibitor] vs. normalized response with variable slope, and their relationship was analyzed using linear regression (R^2 = 0.7973) and Spearman rank correlation coefficient (ρ = 0.9231, p < 0.0001) **(B)**. IC_{50} values could not be interpolated with confidence from "low potency" samples, and as such, were excluded from the correlation.

Measurement of neutralization potency and antibody titers in COVID-19 convalescent patient sera

Using our ELISA neutralization test, we measured the neutralization potency of serum samples from a cohort of convalescent patients with a confirmed COVID-19 diagnosis by qPCR (n = 310). In parallel, we measured the titers of IgG, IgM, and IgA against RBD, spike, and protein N using a direct ELISA approach (Figure 4), which was published recently[19]. The neutralization potency, expressed as the IC_{50}, was strongly correlated to the IgG titers against RBD and spike (ρ = 0.8291 and 0.8297 respectively, p < 0.0001) and to a lower extent with the IgG titers against protein N (ρ = 0.6471, p < 0.0001). Weaker correlations, albeit statistically significant, were found for the IgM and IgA titers against all three viral antigens.

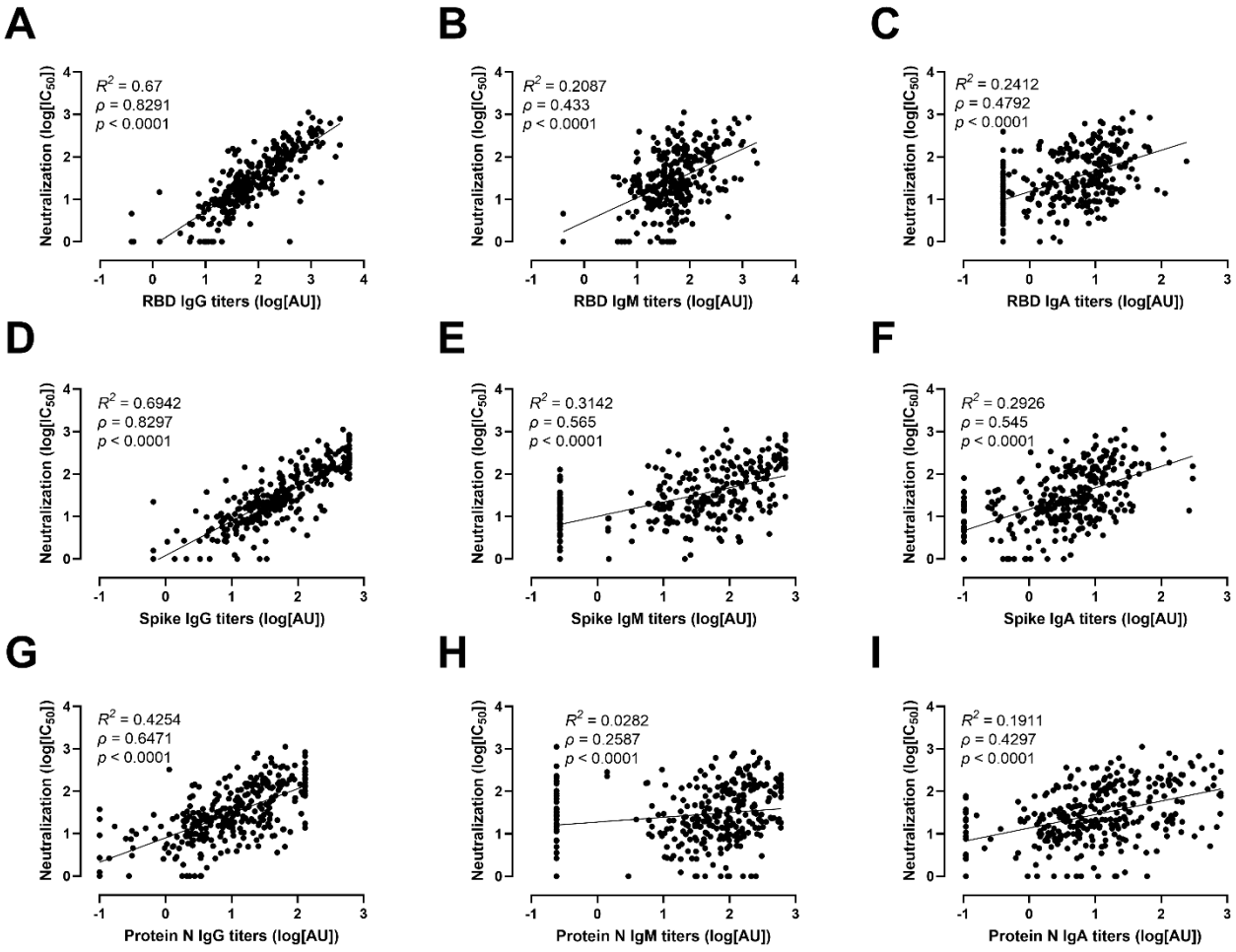

Figure 4. Neutralization potency and antibody titers in COVID-19 convalescent patient sera. Spearman rank correlation and linear regression analyses of the neutralization potency of sera and titers of IgG **(A, D, G)**, IgM **(B, E, H)**, and IgA **(C, F, I)** against RBD **(A–C)**, spike **(D–F)**, and protein N **(G–I).** Trend lines represent linear regression.

Mice immunizations

Next, we evaluated the antibody response in a pre-clinical animal vaccine model. Mice were immunized four times subcutaneously with either the RBD or trimeric spike ectodomain. Each mouse was bled seven days after the second, third and fourth immunization followed by an assessment of the polyclonal response against the antigen. The polyclonal antibody titers against RBD and spike from the third immunization round using a direct ELISA are shown in Figure 5 A and B. The spike-specific antibodies in the RBD and spike immunized mice groups mirrored each other, while the RBD-specific antibody levels were lower in the spike-immunized group. A

SARS-CoV-2 non-related immunized mouse group was used as a negative control. Compared to the antibody titers developed in COVID-19 convalescent individuals—grouped into high, intermediate, and low titers (as determined by our direct RBD ELISA described above) (Figure 5 C, D)—the immunized mice developed in the order of 9–32-fold and 20–35-fold higher RBD and spike titers, respectively, than any of the convalescent patient groups. Next, we assessed the neutralization potency of immunized mice and convalescent patient sera in our antibody neutralization ELISA (Figure 5 E, F), showing that immunized mice, particularly in the RBD group, developed a robust neutralizing response, which was 500-fold more potent than the highest titer response group of convalescent individuals. Antibody titers and neutralization potency of mouse sera reached a maximum already after the second round of immunization. The presented data was generated from sera collected after the third immunization.

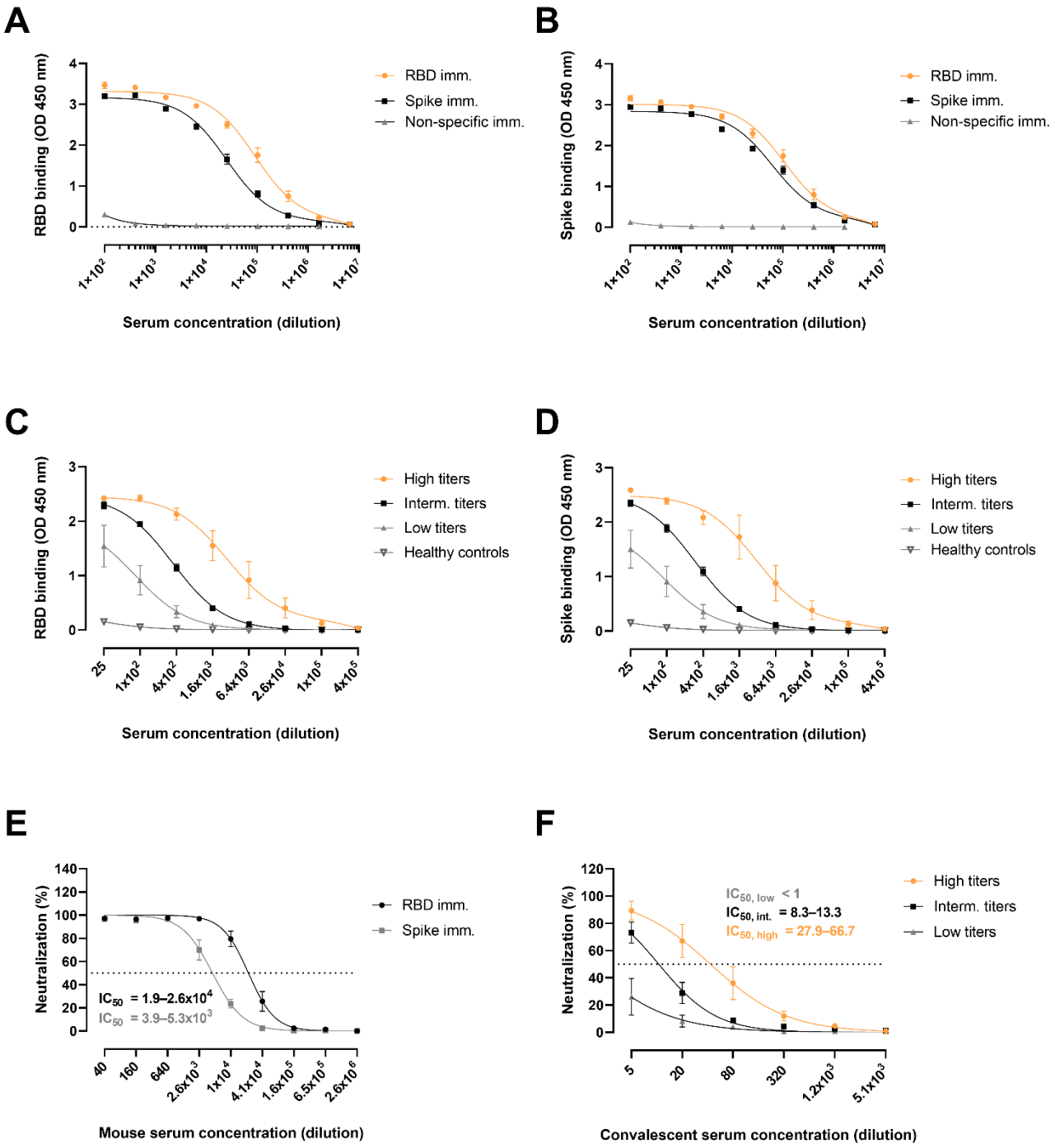

Figure 5. Antibody titers and neutralization potency of polyclonal mouse and convalescent patient sera. Plates coated with recombinant RBD **(A, C)** or spike ectodomain **(B, D)**. Mouse sera from mice immunized with RBD (RBD imm.), spike (Spike imm.), or a SARS-CoV-2 non-related antigen (Non-specific imm.) applied in a 4-fold dilution ($n = 4$ per group) **(A, B)**. Human convalescent sera with high,

intermediate, and low RBD-specific IgG titers were applied in a 4-fold dilution ($n = 4$ per group) **(C, D)**. Serum samples from healthy blood donors were used as negative controls ($n = 4$). Neutralization potency of polyclonal sera from mice immunized with RBD (RBD. imm.) or spike ectodomain (Spike imm.) using our antibody neutralization ELISA ($n = 4$ per group) **(E)**. Connecting lines represent a non-linear fit using the equation one site – total binding. Neutralization potency of human convalescent sera grouped by RBD-specific IgG titers ($n = 5$ per group) **(F)**. Connecting lines represent a non-linear fit using the equation [inhibitor] vs normalized response with variable slope. Data are presented as mean ± SEM. IC_{50} values are reported as 95% asymmetrical confidence intervals.

Development of potent neutralizing mAbs

In the light of the promising results with the polyclonal mice sera, we sought to isolate and characterize potent murine mAbs. We selected and characterized 17 mAbs immunized with RBD and 32 mAbs using trimeric full-length trimeric spike protein ectodomain as antigens and a selected group of these were purified by affinity chromatography. All clones isolated from RBD-immunized mice reacted with RBD and spike to the same extent. However, for the clones that originated from spike immunized mice only 3 out of 32 mAbs showed full RBD:ACE2 inhibition, whereas 9 out of 17 of the mAbs from the RBD immunization showed a strong inhibition profile. In the neutralization assessment, we selected mAbs with a high binding capacity to the RBD (a total of three mAbs from the spike and seven from the RBD immunization). These were further characterized in terms of biochemical and neutralization properties (Figure 6). First, we studied their binding properties using biolayer interferometry (BLI) (Figure 6 A, B). The mAbs were immobilized onto biosensor tips and dipped into wells containing two-fold dilution series of RBD (200–0.4 nM). All antibodies bound to RBD with low nM ($n = 4$) or sub nM affinity ($n = 5$). Epitope binning experiments revealed several epitope hotspots within the RBD, one recognized by RBD clones 1 and 28, and a second recognized by four RBD (15, 26, 30, 31) and one spike clones (53), with RBD clone 5 partially overlapping the same region of RBD clone 15 (Figure 6 B). A third region was located in the spike protein and did not appear to be involved in the interaction with the ACE-2 receptor. Next, we assessed the neutralization potency of the mAbs both in the PRNT (Figure 6 C) and in the antibody neutralization ELISA (Figure 6 D). In Figure 6 C and D, 3 mAbs are illustrated, i.e. two targeting a common epitope within the RBD, and one outside. All seven RBD mAbs were neutralizing, with IC_{50} values ranging from 2 to 20 µg/ml. Of the three spike mAbs, the two mapping outside the RBD were non-neutralizing, while spike clone 53 outperformed all others with an estimated IC_{50} of 0.2–0.3 µg/ml. Binding affinities towards RBD (KD) were not directly correlated with neutralization potency (Figure 6 D).

A

MAb clone	KD (M)	Ka (1/Ms)	Kdis (1/s)
RBD 1	1.36×10^{-10}	6.19×10^{6}	8.4×10^{-4}
RBD 5	3.36×10^{-9}	1.05×10^{6}	3.53×10^{-3}
RBD 15	2.36×10^{-9}	7.23×10^{5}	1.71×10^{-3}
RBD 26	7.19×10^{-10}	4.34×10^{5}	3.12×10^{-4}
RBD 28	1.44×10^{-10}	2.2×10^{6}	3.17×10^{-4}
RBD 30	5.29×10^{-10}	1.69×10^{6}	8.95×10^{-4}
RBD 31	1.84×10^{-9}	1.86×10^{5}	3.42×10^{-4}
Spike 43	-	-	-
Spike 53	2.8×10^{-10}	3.66×10^{5}	1.04×10^{-4}
Spike 56	2.06×10^{-9}	1.31×10^{5}	2.70×10^{-4}

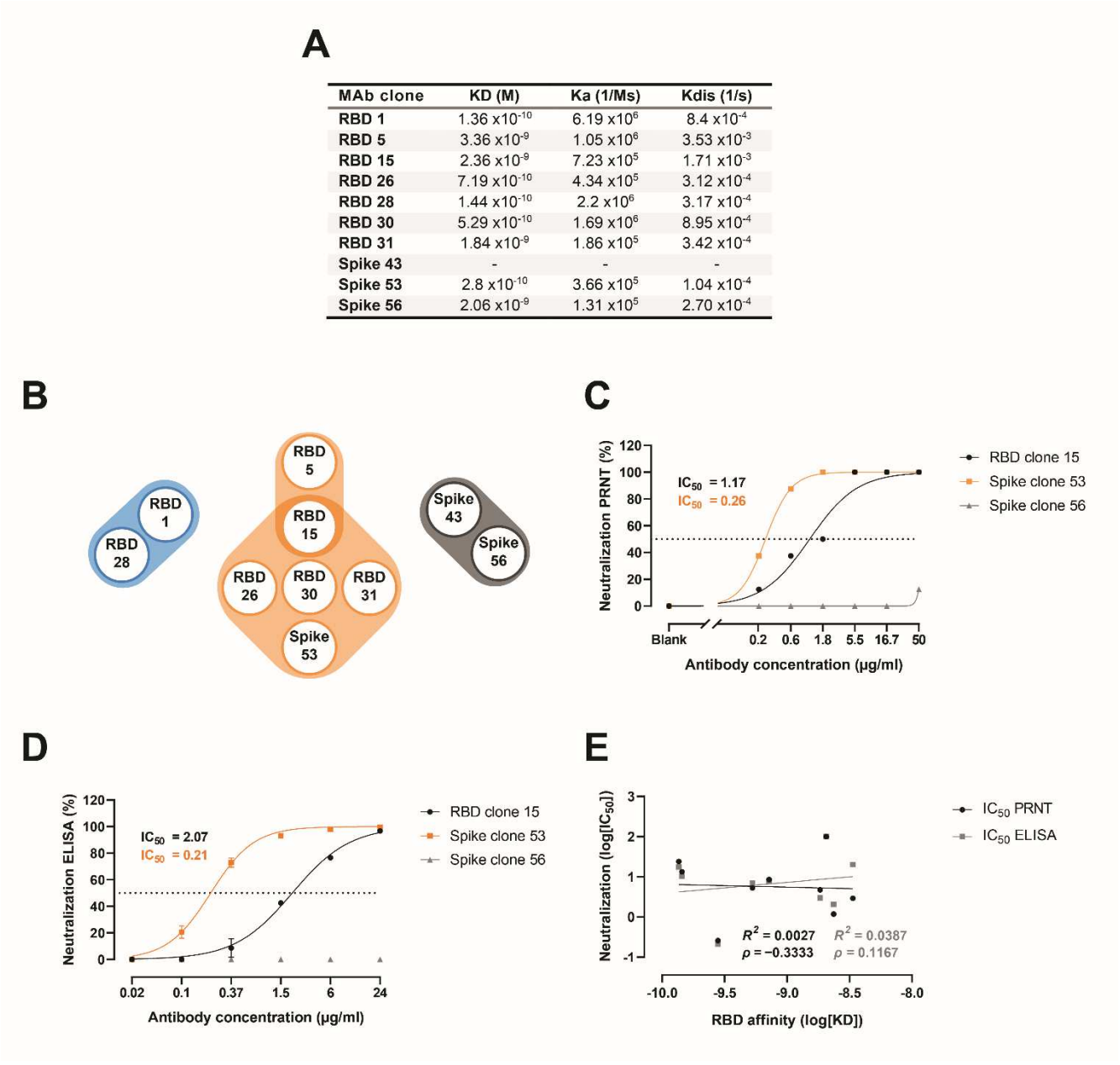

Figure 6. Characterization of SARS-CoV-2 neutralizing mAbs. Binding kinetics of selected mAbs isolated from RBD or spike immunized mice were determined by BLI **(A)**. The antibodies were immobilized in AMC sensors and dipped into serial dilutions of RBD (10-point 2-fold dilution starting at 200 nM). Epitope binning experiments on monomeric spike protein via BLI identified two noncompeting epitopes for both RBD and spike **(B)**. The neutralization potency of three representative high-affinity mAbs was estimated by the PRNT **(C)** and the antibody neutralization ELISA **(D)**. Correlation between the neutralization potencies calculated by the

PRNT and the antibody neutralization ELISA-based test and the dissociation constant (KD) calculated by BLI **(E)**. IC_{50} values from non-neutralizing mAbs were normalized to 100. Non-neutralizing spike clone 43 was excluded from the analysis.Trend line represents the linear regression.

Discussion

There is an urgent need for relevant serological assays to measure the protective effects of the emerging SARS-CoV-2 vaccines. To monitor the prevalence of SARS-CoV-2 exposed individuals in a population, many assays are based either on direct detection of anti-viral antibodies or employing an indirect principle using viral antigens both for capture and detection[28–32]. However, none of these assays measures whether an exposed individual has developed neutralizing protective antibodies. A good alternative would be the PRNT assays. They are considered the gold standard for the evaluation of neutralizing antibody titers. However, PRNT assays are time-consuming, requires high-class biosafety laboratories, have low output and are expensive to perform[15–18]. Because the viral entry of the SARS-CoV-2 to the target cell requires interaction between the RBD domain and the host ACE-2 receptor[33–35], we have developed an fast and simple antibody neutralization ELISA as a proxy for viral neutralization. Using recombinant ectodomains of ACE-2 as capture and biotinylated RBD for detection we were able to establish an antibody inhibition ELISA that correlated highly (ρ = 0.9231, $p < 0.0001$) with the PRNT assay using COVID-19 convalescent sera with a titer spectrum of anti-SARS-CoV-2 antibodies. This suggests that the newly developed antibody neutralization ELISA could replace PRNT and similar assays as a proxy tool to measure antibody-dependent SARS-CoV-2 neutralization. The assay was robust and could be used with various types of analytes (plasma, serum, heat-inactivated serum and purified mAb preparations). Moreover, we could show that the antibody neutralization ELISA correlated well with similar newly launched commercial assays to evaluate viral neutralization. Interestingly, the antibody neutralization ELISA showed a good correlation with IgG antibody levels against SARS-CoV-2 RBD, full-length spike, and protein N, but only a modest correlation with IgA and IgM levels, in agreement with other reports[36].

To mimic a vaccine situation, we tested the ability of the antibody neutralization ELISA to assess the inhibition capacity of sera from mice vaccinated with either recombinant trimeric spike ectodomain or RBD. We performed four rounds of immunization and observed that antibody levels against RBD and spike, as well as neutralization potency, reached a maximum already after the second round, indicating that two immunizations with 14 days interval are sufficient to develop a potent adaptive humoral response. We observed a clear difference in terms of IC_{50} between the neutralization potency of RBD and full-length spike protein immunized mice sera; a much better neutralizing capacity was observed when RBD was used as the immunogen. The reason for this is at present unknown. However, it could imply that the B-cell receptor epitope repertoire is highly distributed on the spike protein surface and that a focused immunization approach using only the RBD might be relevant to consider in future vaccine development strategies. Compatible with such notion is our observation that sera from convalescent

individuals that have been exposed to the whole virus had several hundredfold less neutralizing capacity than the mice immunized with RBD. However, some caution should be taken since we do not know whether the mice response can be directly translated to the human situation. Nevertheless, the results suggest that the RBD without any carrier or other specific formulations could be an excellent vaccine candidate.

To further address whether the antibody neutralization ELISA could be used to monitor monoclonal antibody therapeutics, we developed a panel of mAbs raised against either trimeric ectodomain spike or RBD. These results show that most of the mAbs raised against RBD were indeed virus neutralizing (9 out of 17 with a full inhibition and 5 showed a partial inhibition profile), while a minority of the total number of spike-raised mAbs neutralized the virus (3 out of 32). The mAbs that proved to be of very high affinity (low nM to sub nM KDs) could furthermore be a relevant therapeutic platform to pursue as a neutralizing engineered single-chain variable fragment (scFv) mAb pool capable of inhibiting viral entry without exacerbating the inflammatory response. Moreover, cocktails of noncompeting mAbs can broaden the efficacy of antibody-based treatments by preventing the appearance of potential escape variants, as seen in other viral diseases such as SARS-CoV-1[37] and HIV[38], and providing universal coverage of circulating SARS-CoV-2 isolates.

In conclusion, we have developed a platform to monitor the neutralizing capacity of convalescent plasma meant for COVID-19 therapy, that due to its ease-of-use and safety, could be used in hospitals without access to biosafety level 3 laboratories as a routine test before and after plasmapheresis. Moreover, it can be used as an easy screening platform for selecting the most suitable mAbs for therapeutic development. Probably more important, our platform can be used to monitor the neutralizing humoral vaccine responses towards SARS-Cov-2 safely and on a large scale. Moreover, our data suggest that using RBD as an immunogen compared with full-length spike protein might be a better strategy in creating a robust neutralization antibody response. This should be considered when developing next-generation vaccines against SARS-CoV-2 or related escape strains that could potentially emerge after the present pandemic.

Acknowledgments

The authors would like to thank Camilla Xenia Holtermann Jahn, Sif Kaas Nielsen, and Jytte Bryde Clausen, from the Laboratory of Molecular Medicine, for their excellent technical assistance. This work was financially supported grants from the Carlsberg Foundation (CF20-0045), the Novo Nordisk Foundation (NFF205A0063505 and NNF20SA0064201), and Independent Research Fund Denmark (0214-00001B).

Authors' contributions

RB-O, M-OS and PG conceived and designed the study; RB-O, CH, MS, TB-T, JGJ enabled recombinant protein production; RB-O, MI, AR, LP-A, CBH, CH, LBJ, SRP, MOS performed experiments; RB-O, MI, LP-A, LBJ, SRP analyzed the data; RB-O, MOS and PG wrote the paper with inputs from all co-authors. All authors approved the final version of the manuscript.

References

1. Le TT, Cramer JP, Chen R, Mayhew S. Evolution of the COVID-19 vaccine development landscape. *Nat Rev Drug Discov*. September 2020. doi:10.1038/d41573-020-00151-8

2. Sajna KV, Kamat S. Antibodies at work in the time of severe acute respiratory syndrome coronavirus 2. *Cytotherapy*. 2020. doi:https://doi.org/10.1016/j.jcyt.2020.08.009

3. Thevarajan I, Nguyen THO, Koutsakos M, et al. Breadth of concomitant immune responses prior to patient recovery: a case report of non-severe COVID-19. *Nat Med*. 2020;26(4):453-455. doi:10.1038/s41591-020-0819-2

4. Ni L, Ye F, Cheng M-L, et al. Detection of SARS-CoV-2-Specific Humoral and Cellular Immunity in COVID-19 Convalescent Individuals. *Immunity*. 2020;52(6):971-977.e3. doi:https://doi.org/10.1016/j.immuni.2020.04.023

5. Suthar MS, Zimmerman MG, Kauffman RC, et al. Rapid Generation of Neutralizing Antibody Responses in COVID-19 Patients. *Cell reports Med*. 2020;1(3):100040. doi:10.1016/j.xcrm.2020.100040

6. Long Q-X, Tang X-J, Shi Q-L, et al. Clinical and immunological assessment of asymptomatic SARS-CoV-2 infections. *Nat Med*. 2020;26(8):1200-1204. doi:10.1038/s41591-020-0965-6

7. Wang X, Guo X, Xin Q, et al. Neutralizing Antibody Responses to Severe Acute Respiratory Syndrome Coronavirus 2 in Coronavirus Disease 2019 Inpatients and Convalescent Patients. *Clin Infect Dis*. June 2020. doi:10.1093/cid/ciaa721

8. Zost SJ, Gilchuk P, Case JB, et al. Potently neutralizing and protective human antibodies against SARS-CoV-2. *Nature*. 2020;584(7821):443-449. doi:10.1038/s41586-020-2548-6

9. Lv Z, Deng Y-Q, Ye Q, et al. Structural basis for neutralization of SARS-CoV-2 and SARS-CoV by a potent therapeutic antibody. *Science (80-)*. 2020;369(6510):1505 LP - 1509. doi:10.1126/science.abc5881

10. Wu Y, Wang F, Shen C, et al. A noncompeting pair of human neutralizing antibodies block COVID-19 virus binding to its receptor ACE2. *Science (80-)*. 2020;368(6496):1274 LP - 1278. doi:10.1126/science.abc2241

11. Liu L, Wang P, Nair MS, et al. Potent neutralizing antibodies against multiple epitopes on SARS-CoV-2 spike. *Nature*. 2020;584(7821):450-456. doi:10.1038/s41586-020-2571-7

12. Cao Y, Su B, Guo X, et al. Potent Neutralizing Antibodies against SARS-CoV-2 Identified by High-Throughput Single-Cell Sequencing of Convalescent Patients' B Cells. *Cell*. 2020;182(1):73-84.e16. doi:https://doi.org/10.1016/j.cell.2020.05.025

13. Chen P, Nirula A, Heller B, et al. SARS-CoV-2 Neutralizing Antibody LY-CoV555 in Outpatients with Covid-19. *N Engl J Med*. October 2020. doi:10.1056/NEJMoa2029849

14. Simonovich VA, Burgos Pratx LD, Scibona P, et al. A Randomized Trial of Convalescent Plasma in Covid-19 Severe Pneumonia. *N Engl J Med*. November 2020. doi:10.1056/NEJMoa2031304

15. Ward BJ, Aouchiche S, Martel N, et al. Measurement of measles virus-specific neutralizing antibodies: evaluation of the syncytium inhibition assay in comparison with the plaque reduction neutralization test. *Diagn Microbiol Infect Dis*. 1999;33(3):147-152. doi:10.1016/s0732-8893(98)00069-8

16. Ratnam S, Gadag V, West R, et al. Comparison of commercial enzyme immunoassay kits with plaque reduction neutralization test for detection of measles virus antibody. *J Clin Microbiol*. 1995;33(4):811 LP - 815. http://jcm.asm.org/content/33/4/811.abstract.

17. Mauldin J, Carbone K, Hsu H, Yolken R, Rubin S. Mumps virus-specific antibody titers from pre-vaccine era sera: comparison of the plaque reduction neutralization assay and enzyme immunoassays. *J Clin Microbiol*. 2005;43(9):4847-4851. doi:10.1128/JCM.43.9.4847-4851.2005

18. Gonçalves G, Cutts F, Forsey T, Andrade HR. Comparison of a commercial enzyme immunoassay with plaque reduction neutralization for maternal and infant measles antibody measurement. *Rev Inst Med Trop Sao Paulo*. 1999;41(1):21-26. doi:10.1590/s0036-46651999000100005

19. Hansen CB, Jarlhelt I, Pérez-Alós L, et al. SARS-CoV-2 Antibody Responses Are Correlated to Disease Severity in COVID-19 Convalescent Individuals. *J Immunol*. November 2020:ji2000898. doi:10.4049/jimmunol.2000898

20. Wrapp D, Wang N, Corbett KS, et al. *Cryo-EM Structure of the 2019-NCoV Spike in the Prefusion Conformation*.; 2019. http://science.sciencemag.org/.

21. Jung S-K, McDonald K. Visual gene developer: a fully programmable bioinformatics software for synthetic gene optimization. *BMC Bioinformatics*. 2011;12(1):340. doi:10.1186/1471-2105-12-340

22. Hoffmann M, Kleine-Weber H, Schroeder S, et al. SARS-CoV-2 Cell Entry Depends on ACE2 and TMPRSS2 and Is Blocked by a Clinically Proven Protease Inhibitor. *Cell*. 2020;181(2):271-280.e8. doi:https://doi.org/10.1016/j.cell.2020.02.052

23. Reed, L.J.; Muench H. A simple method of estimating fifty percent endpoints. *Am J Hugiene*. 1938;27:493-497.

24. Skjoedt M-O, Palarasah Y, Rasmussen K, et al. Two mannose-binding lectin homologues and an MBL-associated serine protease are expressed in the gut epithelia of the urochordate species Ciona intestinalis. *Dev Comp Immunol*. 2010;34(1):59-68. doi:10.1016/j.dci.2009.08.004

25. Yu A, Pak AJ, He P, et al. A Multiscale Coarse-grained Model of the SARS-CoV-2 Virion. *Biophys J*. November 2020. doi:10.1016/j.bpj.2020.10.048

26. Yan R, Zhang Y, Li Y, Xia L, Guo Y, Zhou Q. Structural basis for the recognition of SARS-CoV-2 by full-length human ACE2. *Science (80-)*. 2020;367(6485):1444 LP - 1448. doi:10.1126/science.abb2762

27. Saphire EO, Parren PW, Pantophlet R, et al. Crystal structure of a neutralizing human IGG against HIV-1: a template for vaccine design. *Science*. 2001;293(5532):1155-1159. doi:10.1126/science.1061692

28. Luchsinger LL, Ransegnola B, Jin D, et al. Serological Assays Estimate Highly Variable SARS-CoV-2 Neutralizing Antibody Activity in Recovered COVID19 Patients. *J Clin Microbiol*. September 2020:JCM.02005-20. doi:10.1128/JCM.02005-20

29. Okba NMA, Müller MA, Li W, et al. Severe Acute Respiratory Syndrome Coronavirus 2-Specific Antibody Responses in Coronavirus Disease Patients. *Emerg Infect Dis*. 2020;26(7):1478-1488. doi:10.3201/eid2607.200841

30. Amanat F, Stadlbauer D, Strohmeier S, et al. A serological assay to detect SARS-CoV-2 seroconversion in humans. *Nat Med*. 2020;26(7):1033-1036. doi:10.1038/s41591-020-0913-5

31. Wang Y, Zhang L, Sang L, et al. Kinetics of viral load and antibody response in relation to COVID-19 severity. *J Clin Invest*. 2020;130(10):5235-5244. doi:10.1172/JCI138759

32. Isho B, Abe KT, Zuo M, et al. Mucosal versus systemic antibody responses to SARS-CoV-2 antigens in COVID-19 patients. *medRxiv*. January 2020:2020.08.01.20166553. doi:10.1101/2020.08.01.20166553

33. Hoffmann M, Kleine-Weber H, Schroeder S, et al. SARS-CoV-2 Cell Entry Depends on ACE2 and TMPRSS2 and Is Blocked by a Clinically Proven Protease Inhibitor. *Cell*. March 2020. doi:10.1016/j.cell.2020.02.052

34. Zhou P, Yang X Lou, Wang XG, et al. A pneumonia outbreak associated with a new coronavirus of probable bat origin. *Nature*. 2020;579(7798):270-273. doi:10.1038/s41586-020-2012-7

35. Walls AC, Park YJ, Tortorici MA, Wall A, McGuire AT, Veesler D. Structure, Function, and Antigenicity of the SARS-CoV-2 Spike Glycoprotein. *Cell*. 2020;181(2):281-292.e6. doi:10.1016/j.cell.2020.02.058

585 36. Bošnjak B, Stein SC, Willenzon S, et al. Low serum neutralizing anti-SARS-CoV-2 S antibody
586 levels in mildly affected COVID-19 convalescent patients revealed by two different detection
587 methods. *Cell Mol Immunol*. 2020. doi:10.1038/s41423-020-00573-9

588 37. ter Meulen J, van den Brink EN, Poon LLM, et al. Human Monoclonal Antibody Combination
589 against SARS Coronavirus: Synergy and Coverage of Escape Mutants. *PLOS Med*.
590 2006;3(7):e237. https://doi.org/10.1371/journal.pmed.0030237.

591 38. Caskey M, Schoofs T, Gruell H, et al. Antibody 10-1074 suppresses viremia in HIV-1-infected
592 individuals. *Nat Med*. 2017;23(2):185-191. doi:10.1038/nm.4268

593
594

Figures

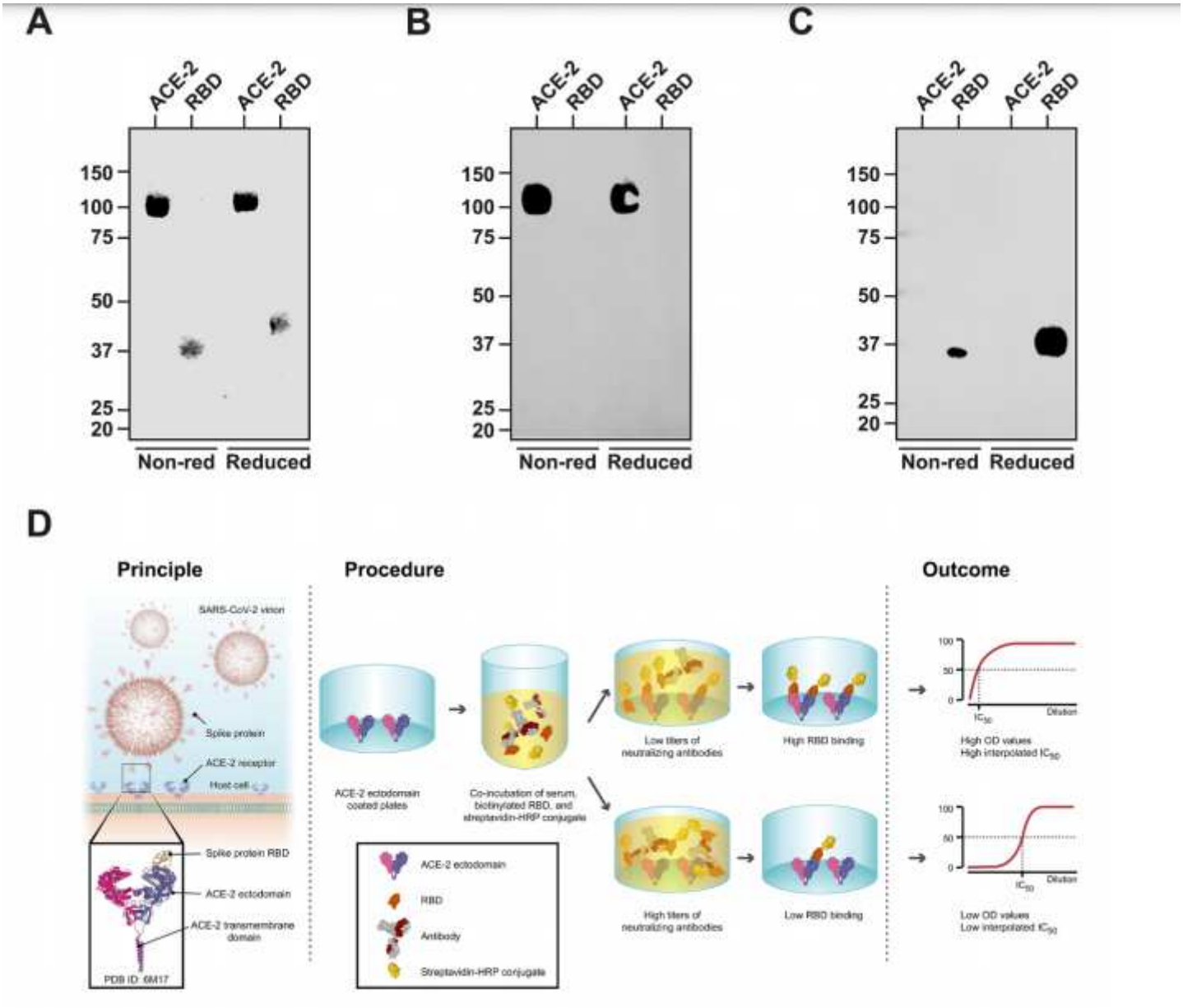

Figure 1

[Please see the manuscript file to view the figure caption.]

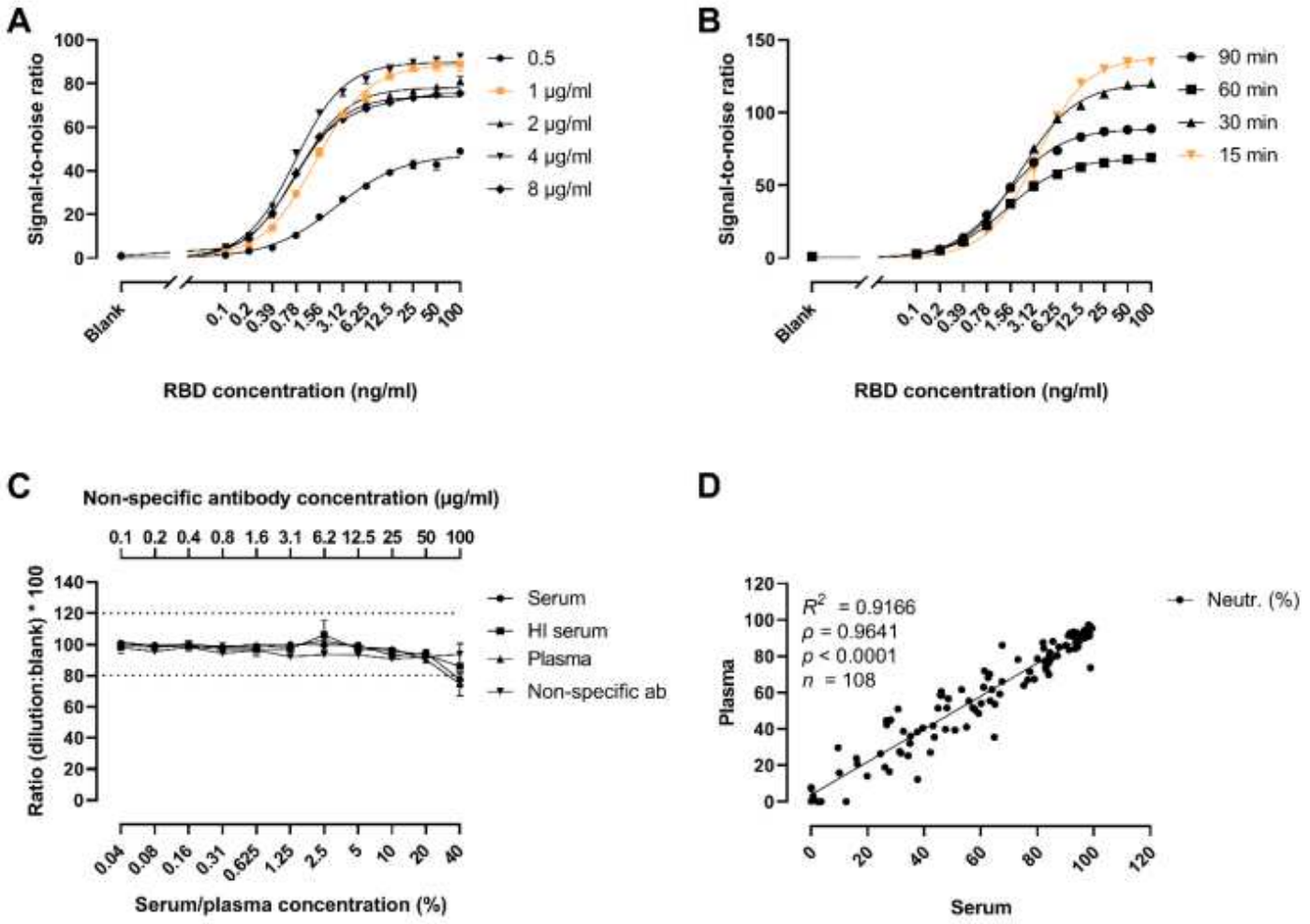

Figure 2

[Please see the manuscript file to view the figure caption.]

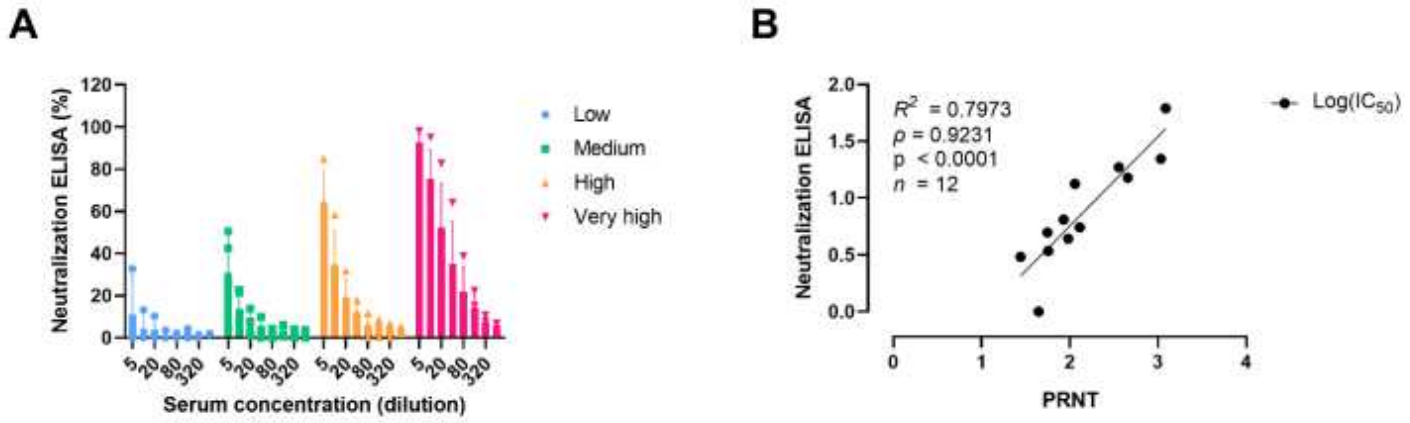

Figure 3

[Please see the manuscript file to view the figure caption.]

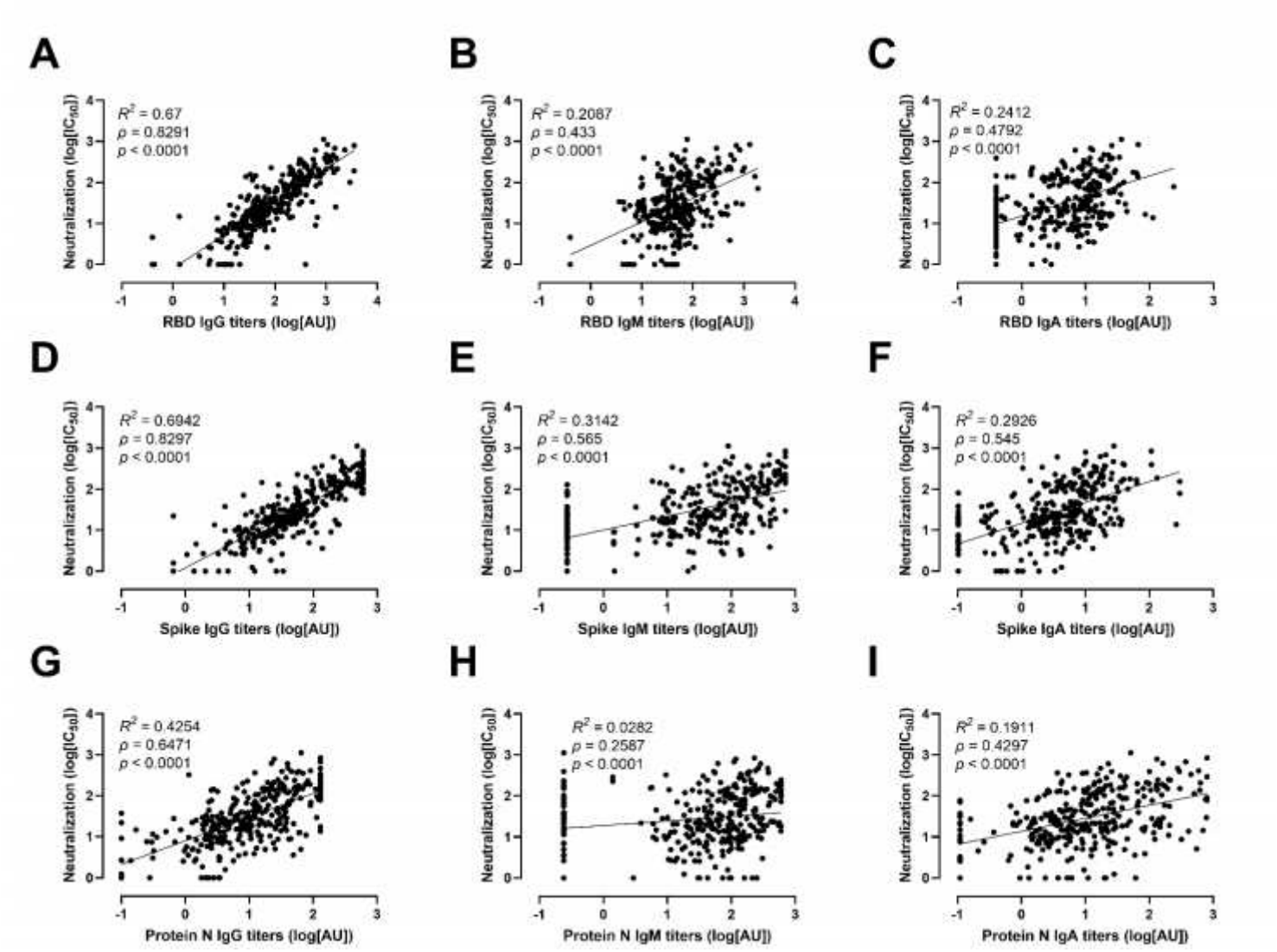

Figure 4

[Please see the manuscript file to view the figure caption.]

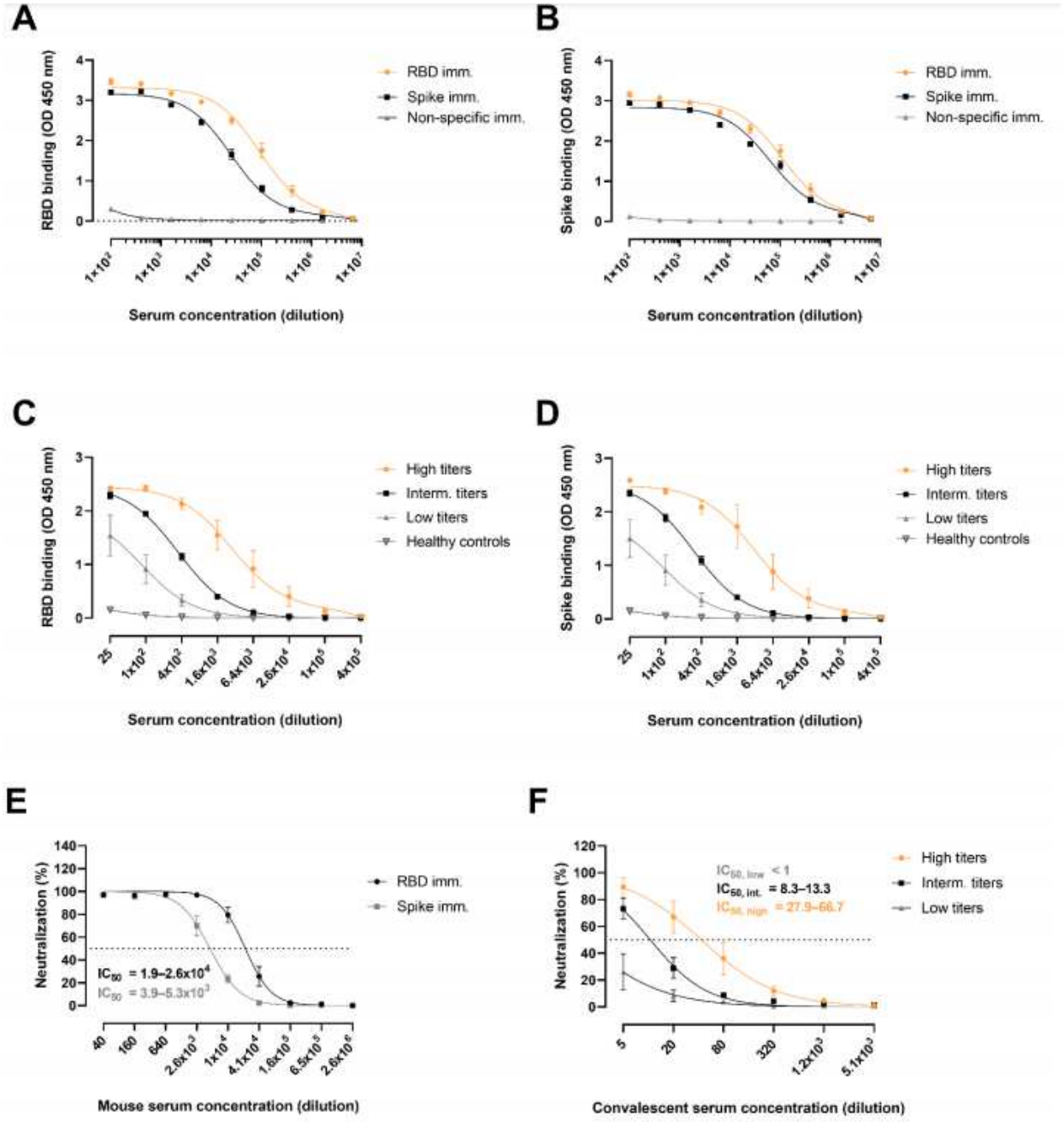

Figure 5

[Please see the manuscript file to view the figure caption.]

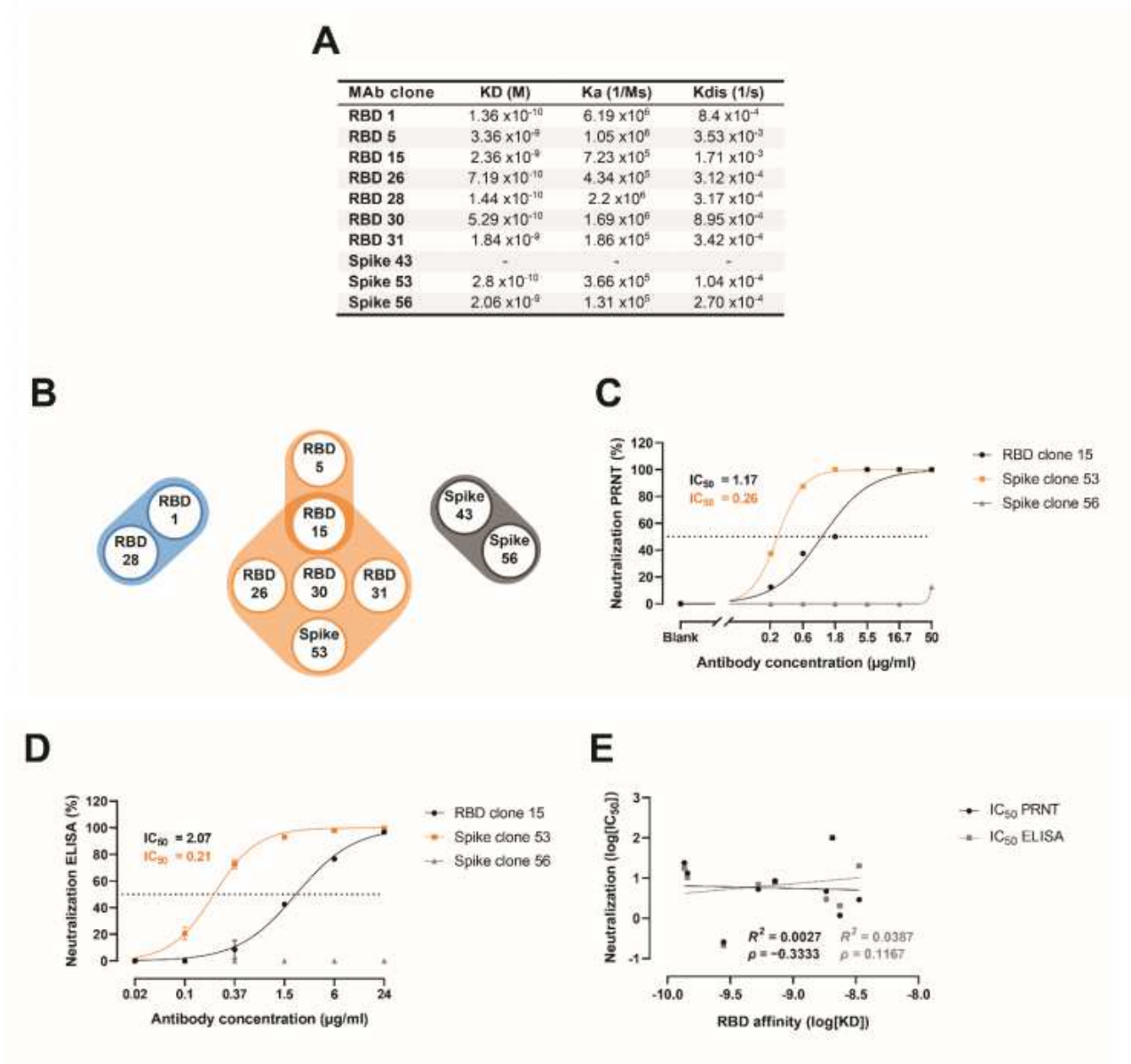

Figure 6

[Please see the manuscript file to view the figure caption.]

Supplementary Files

This is a list of supplementary files associated with this preprint. Click to download.

- Supplementarydata.pdf